Optical and Quantum Electronics (2023) 55:1222
https://doi.org/10.1007/s11082-023-05476-3

Structural, optical and plasmonic sensing characteristics of graphene quantum dots/gold nanolayered film in contact with dopamine solution

Faten Bashar Kamal Eddin[1] · Yap Wing Fen[1,2] · Josephine Ying Chyi Liew[1] · Hong Ngee Lim[3] · Nurul Illya Muhamad Fauzi[2] · Wan Mohd Ebtisyam Mustaqim Mohd Daniyal[2]

Received: 4 June 2023 / Accepted: 22 September 2023 / Published online: 21 October 2023

Abstract

Graphene quantum dots (GQDs) have captured a considerable attention in biomedical field due to their unique structure-related properties. In this work, GQDs monolayer film was coated on gold thin film and integrated into surface plasmon resonance spectroscopy (SPR). The plasmonic sensing properties of GQDs/Au nanostructured layer in contact with varied concentrations of dopamine (DA) solution were evaluated. Increasing DA concentrations increased the changes in the resonance angle. This sensing platform showed a good sensitivity of 0.332°/nM throughout a linear range of 0.01–100 nM, as well as a high binding affinity of 1.610×10^9 M^{-1}. The optical properties of GQDs film were precisely determined by fitting the experimental curves to theoretical data formula using the transfer matrix method (TMM). The fitting results showed that the *n* value of the GQDs film was 1.3049 and its thickness was 7.22 nm in the absence of DA solution. The binding of DA to the SPR chip, as evidenced by the structural analysis of the film using FTIR and AFM, increased the *n* value and thickness of the GQDs film. These findings revealed the obvious changes in the structural and optical characteristics of this GQDs film after interaction with DA, and confirmed the potential of this material in DA sensing when combined with SPR spectroscopy.

Keyword Graphene quantum dots · Neurotransmitters · Surface plasmon resonance · Refractive index sensor · Sensitivity enhancement

✉ Yap Wing Fen
yapwingfen@upm.edu.my

[1] Department of Physics, Faculty of Science, Universiti Putra Malaysia (UPM), 43400 Serdang, Selangor, Malaysia

[2] Functional Nanotechnology Devices Laboratory, Institute of Nanoscience and Nanotechnology (ION2), Universiti Putra Malaysia (UPM), 43400 Serdang, Selangor, Malaysia

[3] Department of Chemistry, Faculty of Science, Universiti Putra Malaysia (UPM), 43400 Serdang, Selangor, Malaysia

1 Introduction

Recently, several studies have revealed that graphene quantum dots (GQDs) films and/or coatings have prospective uses in biomedical (Liu et al. 2017; Qian et al. 2014; Xiao et al. 2016; Li et al. 2017; Zhu et al. 2012a), optical (Zubair et al. 2015; Kim and Kim 2017; Zhang et al. 2018; Tang et al. 2013; Das et al. 2015; Zhu et al. 2012b), and energy applications (Sudhagar et al. 2016; Zhu et al. 2014; Yan et al. 2010a; Majumder et al. 2016; Moon et al. 2017; Protich et al. 2016; Diao et al. 2017), which will influence our quality of life and draw substantial economic interest. The exciton Bohr radius of graphene is infinite (Yan et al. 2010b). GQDs, on the other hand, is a zero-dimensional material obtained by converting two-dimensional graphene. As a result, the quantum confinement and edge effects appeared. Because of the quantum confinement effect, GQDs have several unique features, such as their distinctive fluorescence capabilities found by Pan et al. (2010). If GQDs are to be employed in a variety of applications, the ability to adjust their characteristics is critical. Moreover, GQDs have a high solubility. This is because GQDs have a significant edge effect that may be modified by functional groups. Additionally, GQDs show different chemical and physical characteristics when compared to other carbon-based materials, such as carbon dots, carbon nanotubes, fullerene and graphene (Tian et al. 2018). Along with the structural properties of GQDs thin films, it is critical to precisely characterize the optical properties and thicknesses of GQDs films, on which their appealing qualities depend for their many applications (Sandu 2012; Majhi and Kuiri 2020). Thus far, several approaches have been proposed for this purpose, including laser feedback interferometry (Xu et al. 2014, 2015), ellipsometry (McCrackin et al. 1963; Elizalde et al. 1986; Pristinski et al. 2006), prism coupler (Kirsch 1981; Hou and Mogab 1981; Ding and Garmire 1983), and surface plasmon resonance (SPR) technique (Fen et al. 2011; Rosso et al. 2014; Salvi and Barchiesi 2014; Kamal Eddin et al. 2022a, 2023a; Noda and Hayakawa 2016).

SPR spectroscopy has received significant attention and demonstrated effectiveness as an optical, label-free, and high throughput technique due to its potential for real time detection of heavy metal ions (Lopes et al. 2021; Fen et al. 2013, 2012, 2015; Fen and Yunus 2013a; Fauzi et al. 2020; Ramdzan et al. 2020), glucose (Omidniaee et al. 2022; Rosddi et al. 2021; Panda et al. 2020; Yuan et al. 2018; Kim et al. 2021; Hossain and Talukder 2021; Hakami et al. 2021), DNA (Pal et al. 2018; Haque and Rouf 2021; Shushama et al. 2017; Schneider et al. 2013; Kumar et al. 2019; Azab et al. 2018), hemoglobin (Singh et al. 2021; Mostufa et al. 2021; Sumantri et al. 2020; Mohanty and Sahoo 2016; Heidarzadeh 2020; Duanghathaipornsuk et al. 2020), neurotransmitters (Kamal Eddin et al. 2021, 2022b, c, 2023b; Dutta et al. 2011; Abd Manaf et al. 2017; Yuan et al. 2019), viruses (Omar et al. 2020, 2019; Omar and Fen 2017; Brun et al. 2015; Chang et al. 2018; Cairns et al. 2019; Chung et al. 2005), gases (Nuryadi and Mayasari 2016; Wei et al. 2016; Srivastava et al. 2016), and other targets (Kamal Eddin et al. 2020; García-Aljaro et al. 2008; Verma et al. 2015; Kamalieva et al. 2016) with good reliability and high performance. SPR phenomenon is the oscillation of the charge density at the interface of a metal film and a dielectric (Mao et al. 2015; Maurya et al. 2015; Elmahdy et al. 2022; Singh and Prajapati 2019; Li and Chen 2013; Haiwei et al. 2016; Islam et al. 2021). The high sensitivity of SPR spectroscopy to the boundary conditions enables it to detect the small changes in the medium refractive index induced after the adsorption of the target molecules on the surface of the active layer (Hong et al. 2015; Mukhtar et al. 2016; Xia et al. 2019; Kuo and Chang 2011; Kumar et al. 2021; Elsayed et al. 2017; Zhou et al. 2011). Due to the need to develop the SPR

technique itself, employing the surface plasmons to measure the optical properties as well as the thickness of thin films has gained considerable interest (Bruijn et al. 1990; Hoffmann et al. 1996; Kapoor et al. 2019; Yang et al. 2021; Nur et al. 2019; Kim et al. 2018). Because the reflected light carries information about the used film, the optical properties and thickness of the thin film could only be determined indirectly by mathematical processing of the experimental data (Kamal Eddin et al. 2022a, 2023a; Daniyal et al. 2022; Meradi et al. 2022). Wave propagation in one-dimensional structures may be studied using the transfer matrix method (TMM), which is based on Fresnel's theory. It allows for reflection and transmission computations as well as guided mode evaluations in multilayered systems. TMM treats Fresnel reflection and transmission at the interface of two media as one matrix and light propagation in a particular medium as another. This method provides information on electromagnetic wave propagation through ideal multilayer structures by multiplying matrices (Balili 2012; Tiwari et al. 2015; Chiu et al. 2007; Mudgal et al. 2020; Pandey 2021; Nisha et al. 2019).

In this work, a GQDs/Au nanostructured layer was integrated to SPR spectroscopy to interact with different concentrations of the neurotransmitter dopamine (DA). This was possible due to GQDs' exceptional chemical stability, biocompatibility, and low toxicity, as well as their graphene-like properties, including a substantial surface area and strong surface bonding, making them excellent for diverse biosensing applications (Duhan and Obrai 2023). Furthermore, SPR provides sensitive, real-time, label-free detection of DA. Additionally, unlike electrochemical methods, SPR is less susceptible to interference from other electroactive species. Moreover, it avoids electrode fouling, a common issue that can significantly impact the performance and reliability of electrochemical DA sensing (Kamal Eddin et al. 2022b). This study primarily focused on evaluating the sensor's performance. In addition, the experimentally acquired SPR curves were then computationally processed to analyze the optical properties of the GQDs/Au bilayer structure and determine the thickness of the GQDs film. The reported studies on DA sensors did not investigate DA binding behaviour on the sensor surface using structural measurements. So, the structural analysis of the sensor film prior to and following DA injection was achieved utilizing FTIR spectroscopy and atomic force microscopy (AFM), which confirmed the attachment of DA to GQDs/Au nanostructured layer.

2 Materials and methods

2.1 Materials and reagents

Graphene quantum dots (GQDs) with concentration of 1 mg/mL, and dopamine hydrochloride with molecular weight of 189.64 g/mol were obtained from Sigma-Aldrich. The glass cover slips of 24 × 24 mm with thickness between 0.13 and 0.16 mm and the triangular prism (refractive index of 1.77861) were provided by Menzel-Glaser, Germany. Norland index matching liquid (IML) with refractive index of 1.52 at 589 nm and low viscosity was bought from Norland (USA). This liquid monomer was used to eliminate the reflection losses associated with the glass-air interface. Acetone was used to thoroughly clean the prism and cover slips, assuring that their surfaces were not contaminated and that no leftover adsorbents that may affect the accuracy of the measurements. Throughout experiments, the deionized water (DW) was utilized for dilution.

2.2 Preparation of target solution

To produce 0.5 M of DA solution, 1.896 g of DA powder were dissolved in 20 mL of DW. To dilute DA solution, DW was used to obtain several samples with various low concentrations based on this formula ($M_1V_1 = M_2V_2$).

2.3 Chip modification

The glass cover slip was cleaned with acetone before coating gold thin film on its surface utilizing a K575X sputter coater from Quorum Technologies Ltd (West Sussex, UK). The duration of coating was 67 s using an applied current 20 mA and voltage 2.2 kV. After getting the gold thin films, 0.5 mL of GQDs was distributed evenly on the centre of the gold film's surface. The sensor film (GQDs/Au) was then deposited at high angular velocity of 2000 rpm using spin coating technique (P-6708D). The spin time was 30 s. The prepared GQDs/Au bilayer thin film was left for few hours at room temperature before its incorporation to SPR system.

2.4 Experimental procedure

The sensing performance of GQDs/Au bilayer film towards DA was examined and assessed utilizing a homemade prism based SPR spectroscopy designed in Kretschmann configuration as shown in Fig. 1. The angular interrogation technique was used, where the optical system included a 5 mW He–Ne laser (632.8 nm) with spot diameter of 0.8 mm was employed as excitation source, a light chopper with frequency of 188 Hz, a linear polarizer,

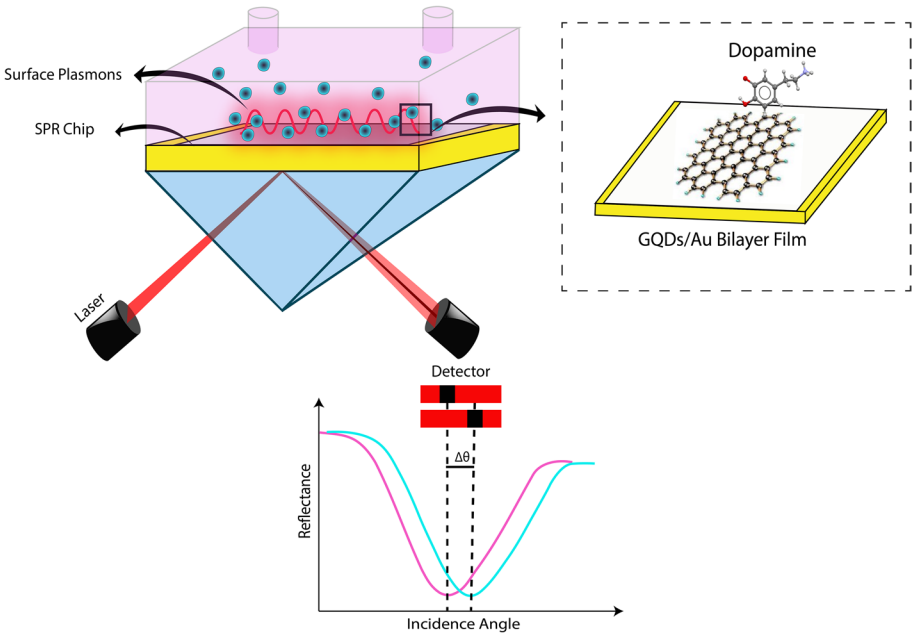

Fig. 1 SPR spectroscopy in Kretschmann configuration

a small pinhole, a prism (triangular with a refractive index of 1.77861), an optical rotating platform powered by a motion controller with a resolution of 0.001° (Newport model MM 3000), a photodetector, as well as a lock-in amplifier. The SPR chips were adherent to the prism side by the index matching liquid and a flow cell containing the target solution contacted the surface of SPR chip. Following that, SPR experiments were performed in the dark. DW was injected into the attached cell to contact the GQDs/Au bilayer film structure and obtain the reference signal. The incidence angles were scanned and the reflectance was measured as a function of incidence angle. As the incidence angle increased to reach the critical angle, the total internal reflection occurred, and the intensity of the reflected light at the interface was around 100%. As the angle increased further, surface plasmons were generated at the interface and the reflected intensity was therefore dropped. The intensity of reflected light from the film surface reached a minimum at the resonance angle. After that, SPR measurements were continued for DA solution of different concentrations.

2.5 Structural analysis techniques

FTIR spectra of GQDs/Au thin film were obtained in the range 400–4000 cm^{-1} utilizing ALPHA II FTIR Spectrometer before and after interactions with DA solution. The FTIR analysis was performed in ATR mode. The topographical measurements of the thin films and the analysis of roughness changes of GQDs films after interaction with DA were done using a Bruker Dimension Edge AFM with 5 μm × 5 μm scanning size. The Peak Force Tapping mode was used with AFM tip's radius of curvature < 10 nm.

3 Result and discussion

3.1 FTIR analysis

FTIR spectrum of GQDs thin film before interaction with DA is shown in Fig. 2 (black spectrum). The peaks appeared at 3848 and 3742 cm^{-1} are attributed to O–H stretching vibration. The peak at 3116 cm^{-1} was attributed to the stretching vibration of O–H and N–H (Teymourinia et al. 2017; Choppadandi et al. 2021). The peaks located around 2882, 2382, 2148, and 2083 cm^{-1} correspond to the stretching vibration of C–H, C=O, C≡C, and C–N, respectively (Ananthanarayanan et al. 2014; Tashkhourian and Dehbozorgi 2016; Wang et al. 2016; Costa et al. 2018; Sadrolhosseini et al. 2020), and the peaks at 2013 and 1768 cm^{-1} were imputed to the stretching of C=O (Teymourinia et al. 2017; Choppadandi et al. 2021; Bokare et al. 2020). The peaks at 1693 and 1528 cm^{-1} were related to the stretching vibrations of C=C and C=O bonds, respectively (Tan et al. 2016; Zhao et al. 2016). The peak centered at 1341 cm^{-1} was assigned to the stretching vibration of C–H and the bending vibration of C–N bond (Tashkhourian and Dehbozorgi 2016; Yuan et al. 2014; Yan et al. 2015), and the peak at 1192 cm^{-1} was attributed to the stretching vibration of C–O bond and the stretching vibrations of C–N groups in amines (Bokare et al. 2020; Abbas et al. 2020). In addition, the peaks appearing at 1079, 1028 and 603 cm^{-1} were due to the stretching vibrations of C–O, C–O–C and bending vibrations of C–H, respectively (Bokare et al. 2020; Zhao et al. 2016; Yan et al. 2015).

After introducing DA, FTIR spectrum recorded for GQDs film (red spectrum) reveals that a few peaks showed a decrease in intensity (3848, 3742, 1528 and 603 cm^{-1}) owing to the overlap with the stretching vibrations of N–H, while the intensity of the peak at 2148

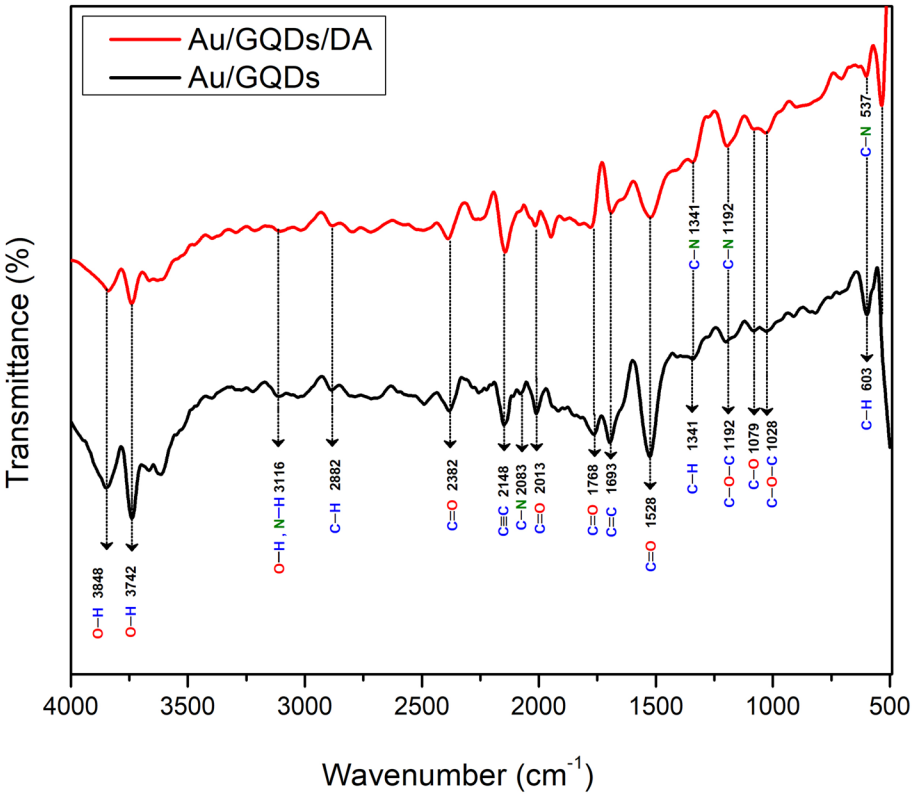

Fig. 2 FTIR spectra of GQDs/Au nanolayered film prior to and following the contact with DA

cm^{-1} was increased. Also, the peaks located at 1341 and 1192 cm^{-1} became more obvious due to C–N stretching vibrations. There was a new peak appeared at 537 cm^{-1} due to the amine C–N stretching (Wang et al. 2016). These results validated the DA-GQDs film interaction and demonstrated that when DA was added, the functional groups of GQDs changed. This confirms that DA was bound to the sensor film's surface and changed its refractive index.

3.2 Surface morphology of GQDs/Au nanolayered film

Before DA injection, the surface morphology of a GQDs film was scanned. The obtained 2D image as shown in Fig. 3a reveals the granular structure and distribution of GQDs on the surface of Au thin film, and the 3D AFM image (Fig. 3c) of GQDs film shows nanoneedles distributed regularly with maximum height of 5.3 nm. However, as shown in Fig. 3b, DA adsorption on the sensor chip affected its granular structure, reducing the number of nanoneedles and decreasing their maximum height to roughly 3.7 nm (Fig. 3d). Furthermore, the sensor surface's average roughness *Ra* was decreased from 0.801 nm to 0.755 nm, and *Rq* was reduced from 1.340 nm to 1.030 nm after DA injection. The considerable change in sensor film morphology and roughness following DA introduction confirms DA binding to GQDs thin film.

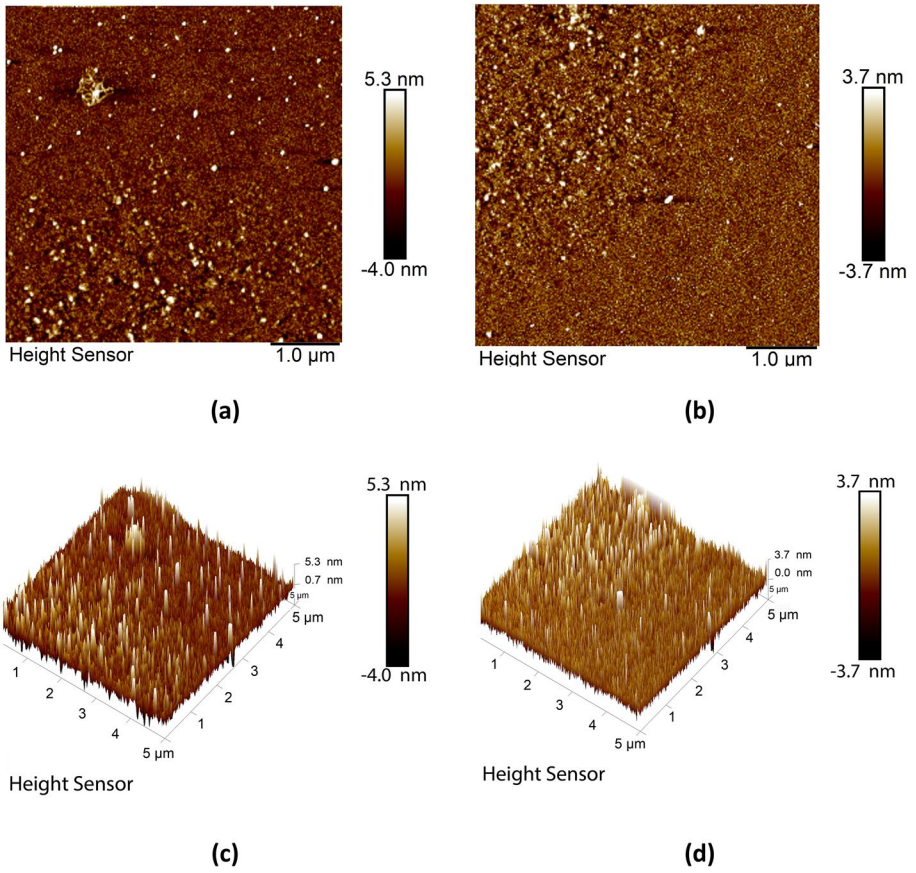

Fig. 3 AFM images of GQDs thin film: (**a**) 2D image before interaction with DA; (**b**) 2D image after interaction with DA; (**c**) 3D image before interaction with DA; and (**d**) 3D image after interaction with DA

3.3 Optical Characterization of GQDs/Au film

The thickness and refractive index of the GQDs/Au nanolayered film were determined through fitting the SPR experimental curves to theoretical data formula using Fresnel's Equation as shown in Fig. 4a–g (Fen and Yunus 2012). The simulation was done based on TMM in MATLAB. In Kretschmann setup, the multilayered structure GQDs/Au was positioned between the triangular prism and the DA solution. At both interfaces where the boundary conditions are met, reflection coefficient r can be expressed by:

$$r = \frac{m_{21} + m_{22}\gamma_2 - m_{11}\gamma_0 - m_{12}\gamma_2\gamma_0}{m_{21} + m_{22}\gamma_2 + m_{11}\gamma_0 + m_{12}\gamma_2\gamma_0} \tag{1}$$

Here m_{11}, m_{12}, m_{21} and m_{22} denote the elements of the transfer matrix, and γ_i can be obtained from the following formula:

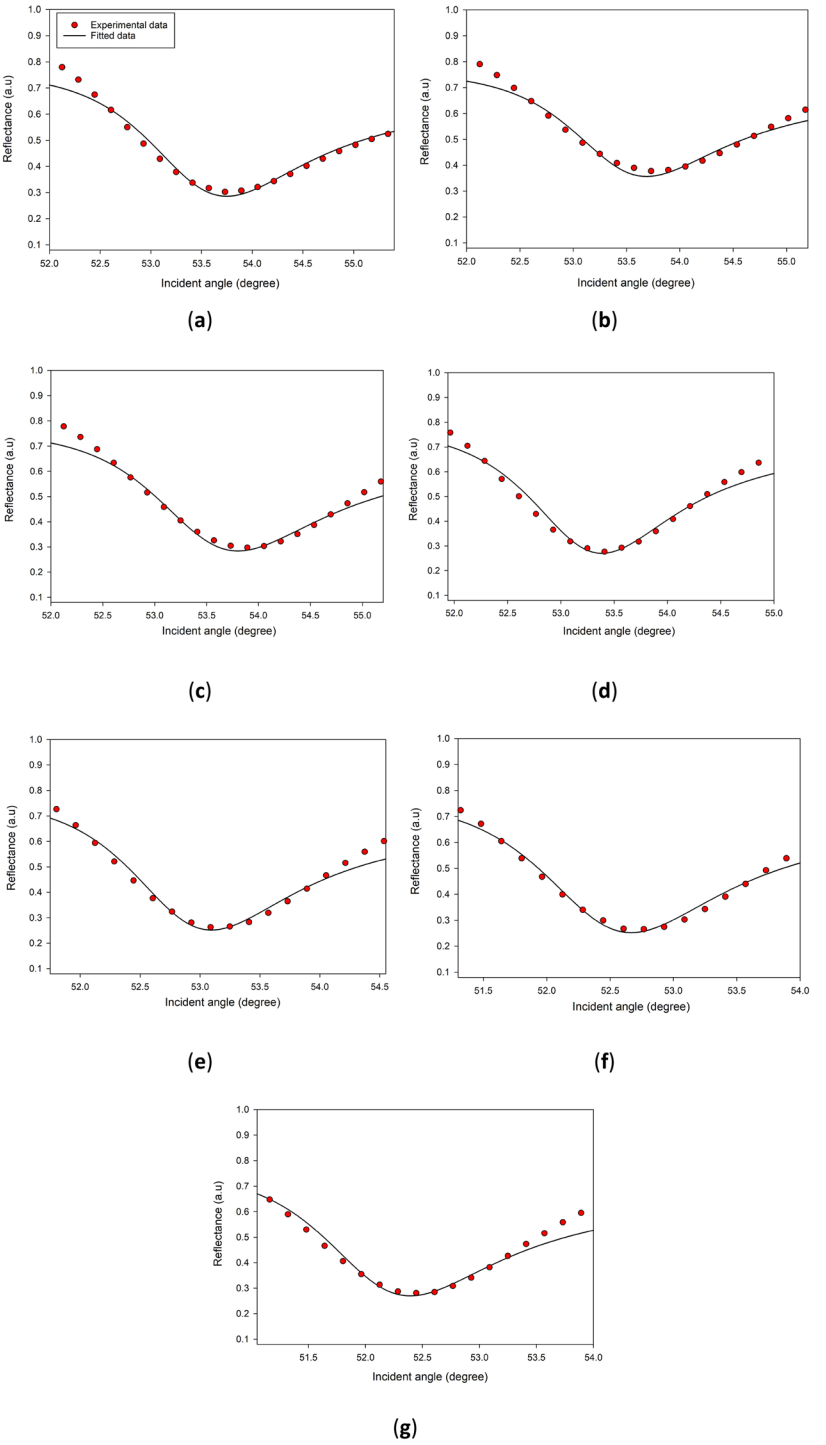

Fig. 4 Fitted and experimental reflectance curves for GQDs/Au nanolayered film exposed to DA solution with concentrations of: (**a**) 0 pM; (**b**) 1 pM; (**c**) 10 pM; (**d**) 100 pM; (**e**) 1 nM; (**f**) 10 nM; and (**g**) 100 nM

$$\gamma_i = \frac{n_i}{\cos(\theta_{ti})}\sqrt{\varepsilon_0\mu_0} \tag{2}$$

where ε_0 and μ_0 are the permittivity and permeability of free space, and i = 0, 1, 2. The reflectivity (R) can be obtained using the formula below:

$$R = rr^* \tag{3}$$

The gold film's refractive index was found to be in good agreement with recent investigations (Fen and Yunus 2013b; Omar et al. 2022), where the n and k were 0.1950 and 3.6820, respectively, and thickness was 57.70 nm. The n and k values of DA solutions were the same as those of DW for concentrations lower than 10 pM. While for higher concentrations, the k value became 0.0030. The fitting yielded the n value of 1.3049 and k value of 0.0000 for GQDs film contacting DW with a thickness of 7.22 nm. As shown in Table 1, the interaction between the sensor chip and DA clearly had an influence on both the n value and the thickness of the GQDs monolayer film. The change in the sensing layer refractive index following contact with varied concentrations of DA solutions was clear through the angular shift of SPR dips.

This table shows the increased change in the n value of GQDs film as DA concentrations rose, which increased the change in the resonance angular shifts. This demonstrates the importance of GQDs thin film in enhancing sensor sensitivity to DA.

3.4 Sensing properties of DA on GQDs film

In our previous work, we have investigated the capability of SPR sensor based on bare gold to detect DA, and our results demonstrated that Au based SPR is insensitive to DA (Omar et al. 2020). Using GQDs/Au thin film, SPR measurements were conducted for DW first, then DA solutions of 1 fM, 1 pM, and 1 nM were introduced one by one into the flow cell to perform measurements and specify the concentration of DA that can be detected by this sensor film. SPR angle was 53.843° when DW contacted GQDs/Au sensing layer. Following that, by inserting DA solution at concentrations of 1 fM and 1 pM, the resonance occurred at 53.843°, the same as with DW. As DA concentration was increased from 1 pM to 1 nM, SPR dip was shifted to the left and the resonance took place at an angle of 53.011°. Because the SPR dip shifted significantly and the angular shift was around 0.830° when DA concentration increased from 1 pM to 1 nM, the measurements were performed for graduated concentrations between 1 pM and 1 nM, and continued for higher

Table 1 Refractive index and thickness values of GQDs monolayer film, the change of the real part of the refractive index Δn, and the resonance angle shift $\Delta\theta$

DA concentration (nM)	n (±0.0001)	k (±0.0001)	d (nm) (±0.01)	Δn
0.000	1.3049	0.0000	7.22	0.0000
0.001	1.3049	0.0000	7.22	0.0000
0.01	1.2758	0.0000	6.83	0.0291
0.1	1.2448	0.0000	6.12	0.0601
1	1.2066	0.0000	5.92	0.0983
10	1.2023	0.0000	4.87	0.1026
100	1.1980	0.0000	4.63	0.1069

Table 2 The resonance angle and angular shift of the SPR dips for GQDs film in contact with DA solutions

DA concentration (nM)	SPR angle (deg)	$\Delta\theta$ (deg)
0.000	53.843	0.000
0.001	53.843	0.000
0.01	53.841	0.002
0.1	53.287	0.556
1	53.011	0.832
10	52.733	1.110
100	52.457	1.386

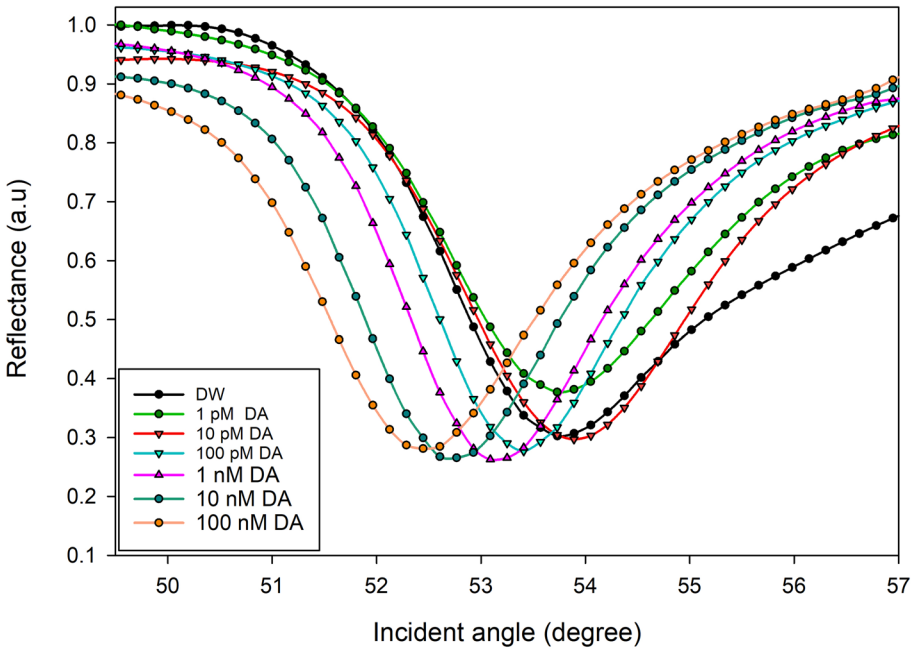

Fig. 5 SPR reflectivity curves acquired experimentally for GQDs/Au nanolayered film subjected to DA solution with concentrations from 1 pM to 100 nM

concentrations, to determine which concentration caused the first shift of the SPR dip. Using another GQDs/Au thin film, the resonance happened at an angle of 53.843° for both DW and 1 pM of DA. When 10 pM of DA was inserted into the attached cell, the SPR dip shifted slightly to lower angle at 53.841°. While, for 100 pM DA, the resonance happened at 53.287° and the angular shift was 0.556° as indicated in Table 2. When DA concentration was raised to 1 nM, the SPR reflectance curve remained shifted by 0.832° from the baseline as shown in Fig. 5. For 10 nM DA, the SPR dip shifted to lower angle of 52.733°. Clearly, the higher concentration of 100 nM of DA solution induced the greatest SPR dip shift of 1.386°.

The correlation between DA concentrations and the resonance angle shift of GQDs/Au based SPR sensor is shown in Fig. 6. The linear fitting yielded a good sensitivity of 0.332°/nM for this GQDs based SPR sensor towards DA ranging from 0.01 to 100 nM, with an R^2

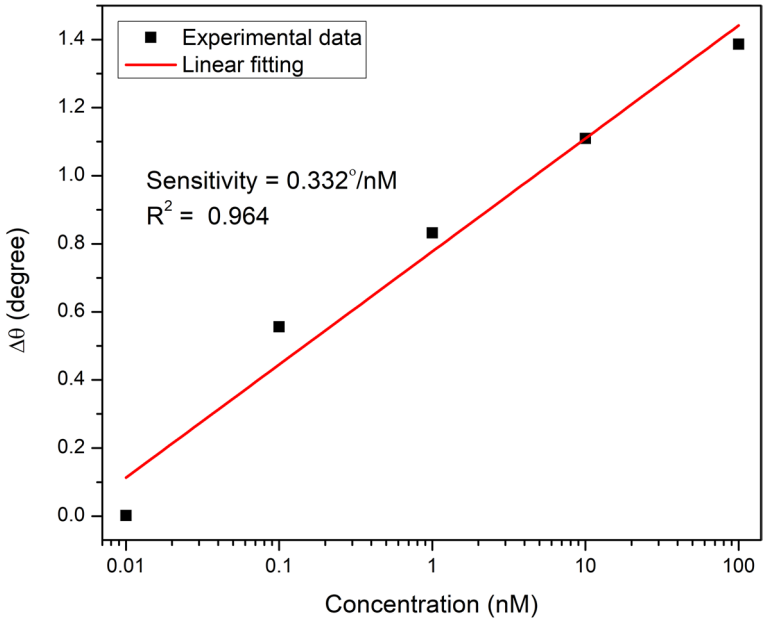

Fig. 6 The linear fitting for the change of resonance angle with DA concentrations

value of 0.964 and a LOD of 0.01 nM. Compared to previous reports on GQDs-based biosensors for DA detection, our sensor has demonstrated the ability to detect even lower concentrations of DA. For instance, Yan et al. (2015) introduced a photoelectrochemical biosensor employing GQDs-TiO_2, which demonstrated acceptable accuracy and precision in DA detection (Yan et al. 2015). Their biosensor exhibited an extensive linear range, spanning from 0.02 to 105 µM, with LOD of 6.7 nM. In the study by Zhou et al. (2015), a fluorescence sensor for DA detection was introduced, utilizing polypyrrole PPy/GQDs core/shell hybrids (Zhou et al. 2015). These composites demonstrated robust fluorescence emission, with an enhancement of up to threefold compared to pristine GQDs. The developed sensor enabled highly sensitive DA determination through a decrease in fluorescent intensity upon the addition of DA. It exhibited excellent linearity within the range of 5–8000 nM, boasting a detection limit of 10 pM. Zhao et al. (2016) presented a fluorescence sensor based on GQDs (Zhao et al. 2016). Their sensor exhibited a linear correlation between quenching efficiency and DA concentration, falling within the range of 0.25–50 µM, with a LOD of 0.09 µM. Pang et al. (2016) employed a hydrothermal method to synthesize graphene quantum dots (GQDs) (Pang et al. 2016). These GQDs were then incorporated into a GQDs-Nafion composite to modify a glassy carbon electrode for use in an electrochemical sensor designed for dopamine (DA) detection. The interaction and electron communication between GQDs and DA were enhanced through π–π stacking forces. Nafion served as an anchoring agent, enhancing the stability and reproducibility of the GQDs on the electrode surface. This GQDs-Nafion composite exhibited a linear detection range spanning from 5 nM to 100 µM, with an LOD of 0.45 nM for DA detection. Baluta et al. (2017) developed a fluorescence-based strategy for DA detection (Baluta et al. 2017). Their approach involved the formation of polydopamine (poly(DA)) on the surface of GQDs and utilized enzyme−laccase for substrate oxidation. Under optimized conditions, this method

exhibited strong analytical performance, featuring high sensitivity and selectivity across a broad linear range. Notably, it achieved a low LOD of 80 nM. The electrochemical sensor developed by Ben Aoun (2017) by modifying a nanostructured carbon screen-printed electrode with a chitosan/nitrogen-doped GQDs nanocomposite exhibited a high sensitivity of 418 μAmM^{-1} cm^{-2} with LOD of 0.145 µM in broad dynamic range (1–200 µM) (Ben Aoun 2017). Arumugasamy et al. (2020) developed a ratiometric electrochemical biosensor using GQDs combined with acid-functionalized multiwall carbon nanotubes (MWCNTs) on a glassy carbon electrode surface (Arumugasamy et al. 2020). Their sensor exhibited good electrocatalytic activity for DA oxidation, covering a dynamic linear range of 0.25–250 µM, with a low detection limit of 95 nM. Chatterjee et al. (2022) synthesized Boron and Sulfur co-doped GQDs (BS-GQDs) and utilized them as a label-free fluorescence-based sensor for the exceptionally sensitive and selective detection of DA. When DA was introduced, BS-GQDs displayed significant fluorescence intensity quenching within a broad concentration range of DA (0–340 µM), achieving LOD of 3.6 µM (Chatterjee et al. 2022). This SPR-based sensor clearly outperforms existing detection methods employing the same material (GQDs) and its composites in constructing the sensing platform.

In order to study the binding affinity of GQDs/Au based sensor towards DA, the nonlinear fitting was applied to the experimental results based on Langmuir and Freundlich isotherm model as shown in Fig. 7. The Langmuir and Freundlich model's equation is as follows (Vijayaraghavan et al. 2006):

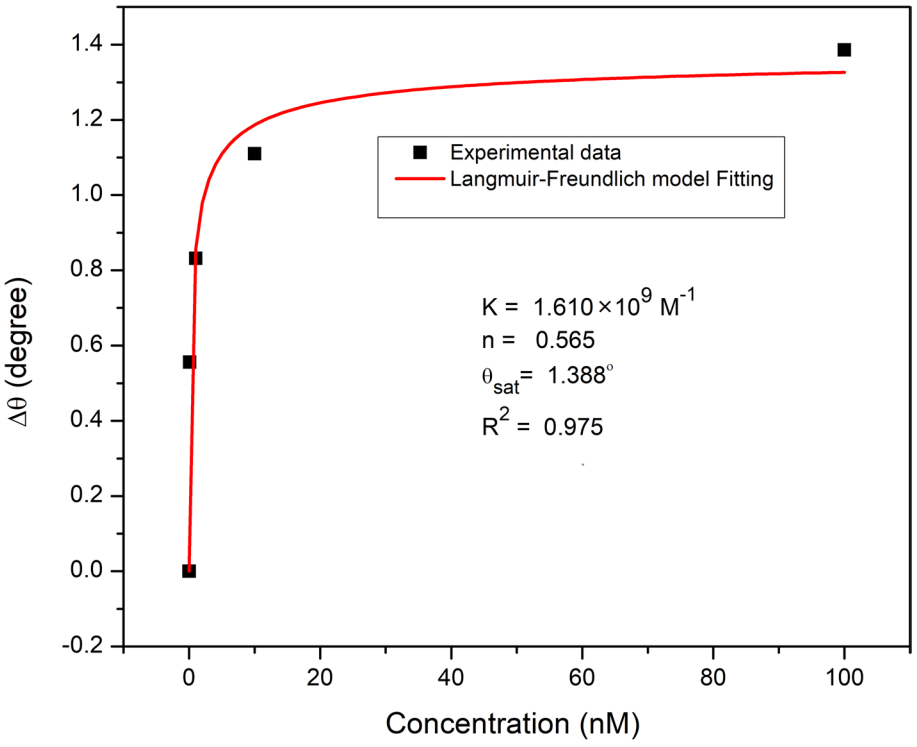

Fig. 7 Experimental and fitting data to Langmuir and Freundlich model for the adsorption of DA on GQDs/Au nanolayered film

$$\Delta\theta = \frac{\Delta\theta_{max} KC^{n}}{1 + KC^{n}} \tag{4}$$

where $\Delta\theta_{max}$ represents the maximum value of the resonance angle shift, K indicates the affinity constant, C is the concentration of the analyte, and n represents the system heterogeneity index.

Langmuir and Freundlich isotherm model was well suited to the experimental results with K value of 1.610×10^{9} M^{-1} and correlation coefficient R^2 of 0.975. Langmuir and Freundlich exponent value was 0.565, and the $\Delta\theta_{max}$ value produced from this model was so close to value obtained experimentally (1.386°).

All SPR curves were fitted to Gaussian model in order to calculate their full width half maximum (FWHM) values. The FWHM value obtained for the reference signal was 3.143° with detection accuracy of 0.318 (deg^{-1}), where the detection accuracy is inversely related to FWHM (Ge et al. 2022). The measurements conducted with DA resulted in SPR curves that were narrower than that for DW, where the obtained value for 1 pM DA was 2.671° as shown in Table 3. This suggests that injecting DA solution to touch the sensor film improved detection accuracy. This might be attributed to sensor film deterioration with increased DA concentrations, which reduced film thickness and FWHM, where the primary resonance experienced a shift. When DA concentrations were increased to 100 pM, the FWHM values continued to fall while the detection accuracy increased to 0.398 (deg^{-1}). The injection of 1 nM DA resulted in an FWHM value of 2.605°, which thereafter dropped to 10 nM. The signal-to-noise ratio (SNR) is calculated by multiplying the resonance angle shift and the detection accuracy (Cennamo et al. 2013; Daniyal et al. 2018). The variation in SNR and detection accuracy values as a function of DA concentrations is shown in Fig. 8. The refractive index of the sensor film significantly changed with increasing DA concentrations, which shifted the SPR dips. As a consequence, the signals noise was decreased and SNR for this sensor were increased.

The strong affinity of DA for the GQDs sensing layer can be attributed to noncovalent interactions between the hydroxyl and carboxyl groups present on the GQDs and the diols, amine functional groups, and phenyl structure in DA. Additionally, π–π stacking forces further bolster the interaction between DA and the GQDs film (Ben Aoun 2017). These combined interactions contribute to the effective detection of DA by this sensor.

Table 3 The values of FWHM, detection accuracy and SNR of the developed sensor

DA Concentration (nM)	FWHM (deg)	Detection accuracy (deg^{-1})	SNR
0.000	3.143	0.318	0.000
0.001	2.671	0.374	0.000
0.01	2.649	0.377	0.001
0.1	2.514	0.398	0.221
1	2.605	0.384	0.319
10	2.496	0.401	0.445
100	2.886	0.347	0.480

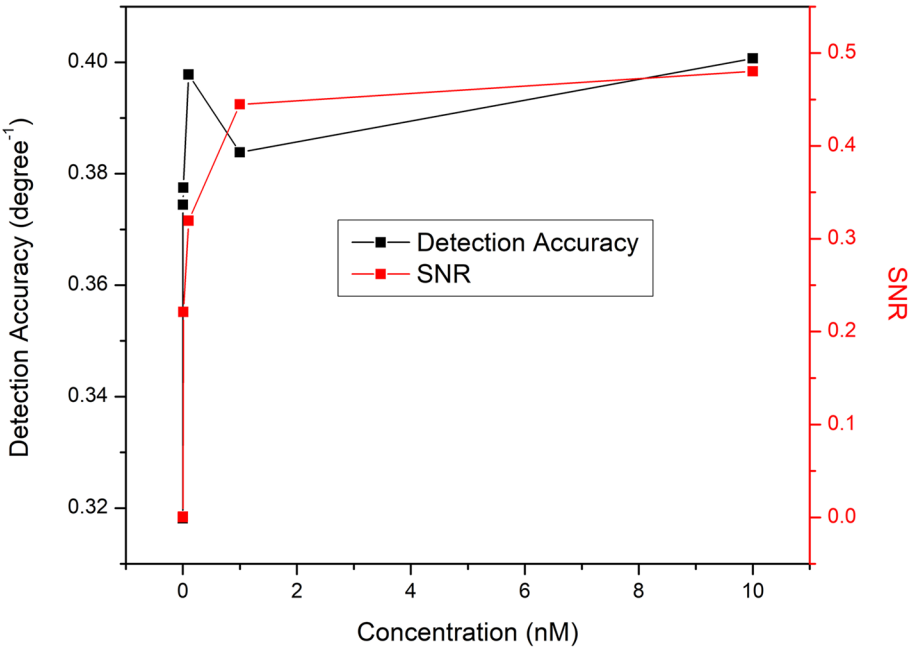

Fig. 8 Variations of the detection accuracy and SNR with DA concentration

4 Conclusions

To conclude, GQDs thin film was prepared and integrated into SPR spectroscopy. Its sensing properties towards DA were investigated for various concentrations of DA solution ranging from 0.01 to 100 nM. Experimentally, the angular shifts of SPR dips were observed when DA concentrations were increased owing to the adsorption of DA on the surface of GQDs film which led to its morphological changes as was verified by FTIR and AFM analysis. The optical properties and thickness of this thin film were determined through fitting the experimental SPR curves to theoretical data based on TMM. This GQDs film combined with the plasmonic based sensing platform proved its efficiency in detecting induced variations in the refractive index of the sensing medium when the thin film was in contact with low concentrations of DA.

Acknowledgements F.B. Kamal Eddin gratefully acknowledges the support received from OWSD and Sida (Swedish International Development Cooperation Agency), the laboratory facilities provided by the Institute of Nanoscience and Nanotechnology, Department of Physics, Department of Chemistry, Universiti Putra Malaysia.

Author contributions Conceptualization, YWF and FBKE; methodology, writing—original draft preparation, FBKE; supervision, validation, funding acquisition, YWF; writing—review and editing, YWF; HNL and FBKE; resources, YWF, JYCL, NIMF and WMEMMD; software, FBKE; visualization, FBKE. All authors have read and agreed to the published version of the manuscript.

Funding This research was funded by the Ministry of Education Malaysia through the Fundamental FRGS (FRGS/1/2019/STG02/UPM/02/1) and Universiti Putra Malaysia through Putra Grant (GP-IPB/2021/9700700).

Data availability All data required to reproduce these findings are included into the paper.

Declarations

Competing interests The authors declare no competing interests.

References

Abbas, A., Tabish, T.A., Bull, S.J., Lim, T.M., Phan, A.N.: High yield synthesis of graphene quantum dots from biomass waste as a highly selective probe for Fe^{3+} sensing. Sci. Rep. **10**, 1–16 (2020). https://doi.org/10.1038/s41598-020-78070-2

Abd Manaf, A., Ghadiry, M., Soltanian, R., Ahmad, H., Lai, C.K.: Picomole dopamine detection using optical chips. Plasmonics **12**, 1505–1510 (2017). https://doi.org/10.1007/s11468-016-0412-1

Ananthanarayanan, A., Wang, X., Routh, P., Sana, B., Lim, S., Kim, D.H., Lim, K.H., Li, J., Chen, P.: Facile synthesis of graphene quantum dots from 3D graphene and their application for Fe^{3+} sensing. Adv. Funct. Mater. **24**, 3021–3026 (2014). https://doi.org/10.1002/adfm.201303441

Arumugasamy, S.K., Govindaraju, S., Yun, K.: Electrochemical sensor for detecting dopamine using graphene quantum dots incorporated with multiwall carbon nanotubes. Appl. Surf. Sci. **508**, 145294 (2020). https://doi.org/10.1016/j.apsusc.2020.145294

Azab, M.Y., Hameed, M.F.O., Nasr, A.M., Obayya, S.S.A.: Label free detection for DNA hybridization using surface plasmon photonic crystal fiber biosensor. Opt. Quantum Electron. **50**, 1–13 (2018). https://doi.org/10.1007/s11082-017-1302-2

Balili, R.B.: Transfer Matrix method in nanophotonics. Int. J. Mod. Phys. Conf. Ser. **17**, 159–168 (2012). https://doi.org/10.1142/s2010194512008057

Baluta, S., Malecha, K., Zając, D., Sołoducho, J., Cabaj, J.: Dopamine sensing with fluorescence strategy based on low temperature co-fired ceramic technology modified with conducting polymers. Sensors Actuators, B Chem. **252**, 803–812 (2017). https://doi.org/10.1016/j.snb.2017.06.073

Ben Aoun, S.: Nanostructured carbon electrode modified with N-doped graphene quantum dots – chitosan nanocomposite : a sensitive electrochemical dopamine sensor. R. Soc. Open Sci. **4**, 1–12 (2017)

Bokare, A., Nordlund, D., Melendrez, C., Robinson, R., Keles, O., Wolcott, A., Erogbogbo, F.: Surface functionality and formation mechanisms of carbon and graphene quantum dots. Diam. Relat. Mater. (2020). https://doi.org/10.1016/j.diamond.2020.108101

Cairns, T.M., Ditto, N.T., Atanasiu, D., Lou, H., Brooks, B.D., Saw, W.T., Eisenberg, R.J., Cohen, G.H.: Surface plasmon resonance reveals direct binding of herpes simplex virus glycoproteins gH/gL to gD and locates a gH/gL binding site on gD. J. Virol. **93**, 1–21 (2019). https://doi.org/10.1128/jvi.00289-19

Cennamo, N., Massarotti, D., Galatus, R., Conte, L., Zeni, L.: Performance comparison of two sensors based on surface plasmon resonance in a plastic optical fiber. Sensors. **13**, 721–735 (2013). https://doi.org/10.3390/s130100721

Chang, Y.F., Wang, W.H., Hong, Y.W., Yuan, R.Y., Chen, K.H., Huang, Y.W., Lu, P.L., Chen, Y.H., Chen, Y.M.A., Su, L.C., Wang, S.F.: Simple strategy for rapid and sensitive detection of avian influenza a H7N9 virus based on intensity-modulated spr biosensor and new generated antibody. Anal. Chem. **90**, 1861–1869 (2018). https://doi.org/10.1021/acs.analchem.7b03934

Chatterjee, M., Nath, P., Kadian, S., Kumar, A., Kumar, V., Roy, P., Manik, G., Satapathi, S.: Highly sensitive and selective detection of dopamine with boron and sulfur co-doped graphene quantum dots. Sci. Rep. **12**, 1–10 (2022). https://doi.org/10.1038/s41598-022-13016-4

Chiu, M.H., Chi, M.H., Shih, C.H.: Optimum sensitivities of D-type optical fiber sensor at a specific incident angle. Appl. Phys. A Mater. Sci. Process. **89**, 413–416 (2007). https://doi.org/10.1007/s00339-007-4136-0

Choppadandi, M., Guduru, A.T., Gondaliya, P., Arya, N., Kalia, K., Kumar, H., Kapusetti, G.: Structural features regulated photoluminescence intensity and cell internalization of carbon and graphene quantum dots for bioimaging. Mater. Sci. Eng. C **129**, 112366 (2021). https://doi.org/10.1016/j.msec.2021.112366

Chung, J.W., Kim, S.D., Bernhardt, R., Pyun, J.C.: Application of SPR biosensor for medical diagnostics of human hepatitis B virus (hHBV. Sens. Actuators, B Chem. **111–112**, 416–422 (2005). https://doi.org/10.1016/j.snb.2005.03.055

da Costa, R.S., da Cunha, W.F., Pereira, N.S., Ceschin, A.M.: An alternative route to obtain carbon quantum dots from photoluminescent materials in peat. Materials. **11**, 12–17 (2018). https://doi.org/10.3390/ma11091492

Daniyal, W.M.E.M.M., Fen, Y.W., Abdullah, J., Sadrolhosseini, A.R., Saleviter, S., Omar, N.A.S.: Exploration of surface plasmon resonance for sensing copper ion based on nanocrystalline cellulose-modified thin film. Opt. Express **26**, 34880 (2018). https://doi.org/10.1364/oe.26.034880

Daniyal, W.M.E.M.M., Fen, Y.W., Kamal Eddin, F.B., Abdullah, J., Mahdi, M.A.: Surface plasmon resonance assisted optical characterization of nickel ion solutionand nanocrystalline cellulose-graphene oxide thin film for sensitivity enhancement analysis. Phys. B Condens. Matter **646**, 414292 (2022). https://doi.org/10.1016/j.physb.2022.414292

Das, S.K., Luk, C.M., Martin, W.E., Tang, L., Kim, D.Y., Lau, S.P., Richards, C.I.: Size and dopant dependent single particle fluorescence properties of graphene quantum dots. J. Phys. Chem. C **31**, 17988–17994 (2015)

de Bruijn, H.E., Kooyman, R.P.H., Greve, J.: Determination of dielectric permittivity and thickness of a metal layer from a surface plasmon resonanceexperiment. Appl. Opt. **29**, 1974 (1990). https://doi.org/10.1364/ao.29.001974

Del Rosso, T., Sánchez, J.E.H., Carvalho, R.D.S., Pandoli, O., Cremona, M.: Accurate and simultaneous measurement of thickness and refractive index of thermally evaporated thin organic films by surface plasmon resonance spectroscopy. Opt. Express **22**, 18914 (2014). https://doi.org/10.1364/oe.22.018914

Diao, S., Zhang, X., Shao, Z., Ding, K., Jie, J., Zhang, X.: 123.5% efficient graphene quantum dots/silicon heterojunction solar cells using graphene transparent electrode. Nano Energy **31**, 359–366 (2017)

Ding, T.N., Garmire, E.: Measuring refractive index and thickness of thin films: a new technique. Appl. Opt. **22**, 3177 (1983). https://doi.org/10.1364/ao.22.003177

Duanghathaipornsuk, S., Shen, B., Cameron, B.D., Ijäs, H., Linko, V., Kostiainen, M.A., Kim, D.S.: Aptamer-embedded DNA origami cage for detecting (glycated) hemoglobin with a surface plasmon resonance sensor. Mater. Lett. **275**, 128141 (2020). https://doi.org/10.1016/j.matlet.2020.128141

Duhan, J., Obrai, S.: Highly sensitive and selective fluorescence and smartphone-based sensor for detection of L-dopa usinga nitrogen sulphur graphene quantum dots. Microchem. J. **193**, 109262 (2023). https://doi.org/10.1016/j.microc.2023.109262

Dutta, P., Pernites, R.B., Danda, C., Advincula, R.C.: SPR detection of dopamine using cathodically electropolymerized, molecularly imprinted poly-p-aminostyrene thin films. Macromol. Chem. Phys. **212**, 2439–2451 (2011). https://doi.org/10.1002/macp.201100365

Elizalde, E., Frigerio, J.M., Rivory, J.: Determination of thickness and optical constants of thin films from photometric and ellipsometric measurements. Appl. Opt. **25**, 4557 (1986). https://doi.org/10.1364/ao.25.004557

Elmahdy, N.A., Hameed, M.F.O., Obayya, S.S.A.: Refractive index sensor based on plasmonic D-shaped photonic crystal fiber with pyramid grating. Opt. Quantum Electron. **54**, 1–14 (2022). https://doi.org/10.1007/s11082-022-04102-y

Elsayed, M.Y., Ismail, Y., Swillam, M.A.: Semiconductor plasmonic gas sensor using on-chip infrared spectroscopy. Appl. Phys. A Mater. Sci. Process. **123**, 1–7 (2017). https://doi.org/10.1007/s00339-016-0707-2

Fauzi, N.I.M., Fen, Y.W., Omar, N.A.S., Saleviter, S., Daniyal, W.M.E.M.M., Hashim, H.S., Nasrullah, M.: Nanostructured chitosan/maghemite composites thin film for potential optical detection of mercury ion by surface plasmon resonance investigation. Polymers **12**, 1497 (2020)

Fen, Y.W., Yunus, W.M.M.: Optical characterization of multi layer thin films using surface plasmon resonance method: from electromagnetic theory to sensor application. AIP Conf. Proc. **1482**, 132–135 (2012). https://doi.org/10.1063/1.4757452

Fen, Y.W., Yunus, W.M.M.: Surface plasmon resonance spectroscopy as an alternative for sensing heavy metal ions: a review. Sens. Rev. **33**, 305–314 (2013a)

Fen, Y.W., Yunus, W.M.M.: Utilization of chitosan-based sensor thin films for the detection of lead ion by surface plasmon resonance optical sensor. IEEE Sens. J. **13**, 1413–1418 (2013b)

Fen, Y.W., Yunus, W.M.M., Yusof, N.A.: Detection of mercury and copper ions using surface plasmon resonance optical sensor. Sensors Mater. **23**, 325–334 (2011). https://doi.org/10.18494/sam.2011.723

Fen, Y.W., Mat, W.M., Azah, N.: Surface plasmon resonance optical sensor for detection of Pb^{2+} based on immobilized p-tert-butylcalix [4] arene-tetrakis in chitosan thin film as an active layer. Sens. Actuators, B Chem. **171–172**, 287–293 (2012). https://doi.org/10.1016/j.snb.2012.03.070

Fen, Y.W., Yunus, W.M.M., Talib, Z.A.: Analysis of Pb(II) ion sensing by crosslinked chitosan thin film using surface plasmon resonance spectroscopy. Opt. Int. J. Light Electron Opt. **124**, 126–133 (2013). https://doi.org/10.1016/j.ijleo.2011.11.035

Fen, Y.W., Yunus, W.M.M., Yusof, N.A., Ishak, N.S., Omar, N.A.S., Zainudin, A.A.: Preparation, characterization and optical properties of ionophore doped chitosanbiopolymer thin film and its potential application for sensing metal ion. Optik **126**, 4688–4692 (2015)

García-Aljaro, C., Muñoz-Berbel, X., Jenkins, A.T.A., Blanch, A.R., Muñoz, F.X.: Surface plasmon resonance assay for real-time monitoring of somatic coliphages in wastewaters. Appl. Environ. Microbiol. **74**, 4054–4058 (2008). https://doi.org/10.1128/AEM.02806-07

Ge, D., Zhou, Y., Shi, J., Zhang, L., Zhu, S.: Highly sensitive refractive index sensor based on Bloch surface waves with lithium niobate film. Appl. Phys. A Mater. Sci. Process. **128**, 1–7 (2022). https://doi.org/10.1007/s00339-021-05212-2

Haiwei, M., Jingwei, L., Zhaoting, L., Shijie, Z., Lin, Y., Tao, S., Qiang, L., Chao, L.: Optical properties of local surface plasmon resonance in Ag/ITO sliced nanosphere by the discrete dipole approximation. Appl. Phys. A Mater. Sci. Process. **122**, 1–8 (2016). https://doi.org/10.1007/s00339-016-9954-5

Hakami, J., Abassi, A., Dhibi, A.: Performance enhancement of surface plasmon resonance sensor based on Ag-TiO_2-$MAPbX_3$-graphene for the detection of glucose in water. Opt. Quantum Electron. **53**, 1–17 (2021). https://doi.org/10.1007/s11082-021-02822-1

Haque, T., Rouf, H.K.: DNA hybridization detection using graphene-MoSe2–Ag heterostructure-based surface plasmon resonance biosensor. Appl. Phys. A Mater. Sci. Process. **127**, 1–13 (2021). https://doi.org/10.1007/s00339-021-04888-w

Heidarzadeh, H.: Analysis and simulation of a plasmonic biosensor for hemoglobin concentration detection using noble metal nano-particles resonances. Opt. Commun. **459**, 124940 (2020). https://doi.org/10.1016/j.optcom.2019.124940

Hoffmann, A., Kroo, N., Lenkefi, Z., Szentirmay, Z.: A high precision ATR study of surface plasmon mediated reflectance in noble metal films. Surf. Sci. **352–354**, 1043–1046 (1996). https://doi.org/10.1016/0039-6028(95)01324-5

Hong, L.H., Yahaya, A., Munajat, Y.: Simulation of surface plasmon resonance sensor. AIP Conf. Proc. **1674**, 1–6 (2015). https://doi.org/10.1063/1.4928832

Hossain, M.M., Talukder, M.A.: Gate-controlled graphene surface plasmon resonance glucose sensor. Opt. Commun. **493**, 126994 (2021). https://doi.org/10.1016/j.optcom.2021.126994

Hou, T.W., Mogab, C.J.: Plasma silicon oxide films on garnet substrates: measurement of their thickness and refractive index by the prism coupling technique. Appl. Opt. **20**, 3184 (1981). https://doi.org/10.1364/ao.20.003184

Islam, M.R., Iftekher, A.N.M., Hasan, K.R., Nayen, M.J., Bin Islam, S., Islam, R., Khan, R.L., Moazzam, E., Tasnim, Z.: Surface plasmon resonance based highly sensitive gold coated PCF biosensor. Appl. Phys. A Mater. Sci. Process. **127**, 1–12 (2021). https://doi.org/10.1007/s00339-020-04162-5

Kamal Eddin, F.B., Fen, Y.W.: The principle of nanomaterials based surface plasmon resonance biosensors and its potential for dopamine detection. Molecules **25**, 2769 (2020). https://doi.org/10.3390/molecules25122769

Kamal Eddin, F.B., Fen, Y.W.: Recent advances in electrochemical and optical sensing of dopamine. Sensors **20**, 1039 (2020). https://doi.org/10.3390/s20041039

Kamal Eddin, F.B., Fen, Y.W., Omar, N.A.S., Liew, J.Y.C., Daniyal, W.M.E.M.M.: Femtomolar detection of dopamine using surface plasmon resonance sensor based on chitosan/graphene quantum dots thin film, Spectrochim. Acta Part A Mol. Biomol. Spectrosc. **263**, 120202 (2021). https://doi.org/10.1016/j.saa.2021.120202

Kamal Eddin, F.B., Fen, Y.W., Sadrolhosseini, A.R., Liew, J.Y.C., Mohd Daniyal, W.M.E.M.: Optical property analysis of chitosan - graphene quantum dots thin film and dopamine using surface plasmon resonance spectroscopy. Plasmonics **17**, 1985–1997 (2022a). https://doi.org/10.1007/s11468-022-01680-1

Kamal Eddin, F.B., Fen, Y.W., Illya, M., Fauzi, N., Hashim, H.S., Sadrolhosseini, A.R., Abdullah, H.: Direct and sensitive detection of dopamine using carbonquantum dots based refractive index surface plasmon resonance sensor. Nanomaterials **12**, 1799 (2022b)

Kamal Eddin, F.B., Fen, Y.W., Liew, J.Y.C., Daniyal, W.M.E.M.M.: Plasmonic refractive index sensor enhanced with chitosan/Au bilayer thin film for dopaminedetection. Biosensors **12**, 1124 (2022c)

Kamal Eddin, F.B., Fen, Y.W., Liew, J.Y.C., Lim, H.N., Daniyal, W.M.E.M.M., Omar, N.A.S.: Simultaneous measurement of the refractive index and thickness of graphene oxide/gold multilayered structure for potential in dopamine sensing using surface plasmon resonance spectroscopy. Optik **278**, 170703 (2023a). https://doi.org/10.1016/j.ijleo.2023.170703

Kamal Eddin, F.B., Fen, Y.W., Liew, J.Y.C., Fauzi, N.I.M., Daniyal, W.M.E.M.M., Abdullah, H.: Development of plasmonic-based sensor for highly sensitive and selective detection of dopamine. Opt. Laser Technol. **161**, 109221 (2023b). https://doi.org/10.1016/j.optlastec.2023.109221

Kamalieva, A., Toropov, N., Reznik, I., Vartanyan, T.: Plasmon-assisted aggregation and spectral modification of the layered rhodamine 6G molecules. Opt. Quantum Electron. **48**, 1–8 (2016). https://doi.org/10.1007/s11082-016-0841-2

Kapoor, V., Sharma, N.K., Sajal, V.: Indium tin oxide and silver based fiber optic SPR sensor: an experimental study. Opt. Quantum Electron. **51**, 1–7 (2019). https://doi.org/10.1007/s11082-019-1837-5

Kim, D.H., Kim, T.W.: Ultrahigh current efficiency of light-emitting devices based on octadecylamine-graphene quantum dots. Nano Energy **32**, 441–447 (2017)
Kim, D.G., Kim, S.H., Ki, H.C., Kim, T.U., Shin, J.C., Choi, Y.W.: Resonance characteristics of localized plasmonic structures with periodic ZnO nano-patterns. Opt. Quantum Electron. **50**, 1–9 (2018). https://doi.org/10.1007/s11082-018-1605-y
Kim, H.M., Kim, W.J., Kim, K.O., Park, J.H., Lee, S.K.: Performance improvement of a glucose sensor based on fiber optic localized surface plasmon resonance and anti-aggregation of the non-enzymatic receptor. J. Alloys Compd. **884**, 161140 (2021). https://doi.org/10.1016/j.jallcom.2021.161140
Kirsch, S.T.: Determining the refractive index and thickness of thin films from prism coupler measurements. Appl. Opt. **20**, 2085–2089 (1981)
Kumar, Y., Mishra, R., Panwar, E., Kaur, J., Panwar, R.: Design, optimization and critical analysis of graphene based surface plasmon resonance sensor for DNA hybridization. Opt. Quantum Electron. **51**, 1–12 (2019). https://doi.org/10.1007/s11082-019-2057-8
Kumar, R., Pal, S., Pal, N., Mishra, V., Prajapati, Y.K.: High-performance bimetallic surface plasmon resonance biochemical sensor using a black phosphorus–MXene hybrid structure. Appl. Phys. A Mater. Sci. Process. **127**, 1–12 (2021). https://doi.org/10.1007/s00339-021-04408-w
Kuo, W.K., Chang, C.H.: Experimental comparison between intensity and phase detection sensitivities of grating coupling surface plasmon resonance. Appl. Phys. A Mater. Sci. Process. **104**, 765–768 (2011). https://doi.org/10.1007/s00339-011-6419-8
Le Brun, A.P., Soliakov, A., Shah, D.S.H., Holt, S.A., McGill, A., Lakey, J.H.: Engineered self-assembling monolayers for label free detection of influenza nucleoprotein. Biomed. Micro **17**, 1–10 (2015). https://doi.org/10.1007/s10544-015-9951-z
Li, W., Chen, F.: Effect of transition metal (Fe, Cu, Ni, Rh)-doped small silver chains on optics of plasmon resonances. Appl. Phys. A Mater. Sci. Process. **113**, 543–548 (2013). https://doi.org/10.1007/s00339-013-7842-9
Li, K., Liu, W., Ni, Y., Li, D., Lin, D., Su, Z., Wei, G.: Technical synthesis and biomedical applications of graphene quantum dots. J. Mater. Chem. B **5**, 4811–4826 (2017)
Liu, H., Na, W., Liu, Z., Chen, X., Su, X.: A novel turn-on fluorescent strategy for sensing ascorbic acid using graphene quantum dots as fluorescent probe. Biosens. Bioelectron. **92**, 229–233 (2017)
Lopes, R.B., Junior, D.S., de Silva, F.R.O., Courrol, L.C.: High-sensitivity Hg^{2+} sensor based on the optical properties of silver nanoparticles synthesized with aqueous leaf extract of Mimusops coriacea. Appl. Phys. A Mater. Sci. Process. **127**, 1–13 (2021). https://doi.org/10.1007/s00339-021-04391-2
Majhi, J.K., Kuiri, P.K.: Enhancement of spectral shift of plasmon resonances in bimetallic noble metal nanoparticles in core–shell structure. J. Nanopart. Res. **22**, 86 (2020). https://doi.org/10.1007/s11051-020-4782-0
Majumder, T., Debnath, K., Dhar, S., Hmar, J.J.L., Mondal, S.P.: Nitrogen-doped graphene quantum dot-decorated ZnO nanorods for improved electrochemical solar energy conversion. Energy Technol. **4**, 1–10 (2016)
Mao, P., Luo, Y., Chen, C., Peng, S., Feng, X., Tang, J., Fang, J., Zhang, J., Lu, H., Yu, J., Chen, Z.: Design and optimization of surface plasmon resonance sensor based on multimode fiber. Opt. Quantum Electron. **47**, 1495–1502 (2015). https://doi.org/10.1007/s11082-015-0133-2
Maurya, J.B., Prajapati, Y.K., Singh, V., Saini, J.P., Tripathi, R.: Performance of graphene–MoS_2 based surface plasmon resonance sensor using Silicon layer. Opt. Quantum Electron. **47**, 3599–3611 (2015). https://doi.org/10.1007/s11082-015-0233-z
McCrackin, F.L., Passaglia, E., Stromberg, R.R., Steinberg, H.L.: Measurement of the thickness and refractive index of very thin films and the optical properties of surfaces by ellipsometry. J. Res. Natl. Bur. Stand. A Phys. Chem. **67**, 363–377 (1963). https://doi.org/10.6028/jres.106.025
Meradi, K.A., Tayeboun, F., Guerinik, A., Zaky, Z.A., Aly, A.H.: Optical biosensor based on enhanced surface plasmon resonance: theoretical optimization. Opt. Quantum Electron. **54**, 1–11 (2022). https://doi.org/10.1007/s11082-021-03504-8
Mohanty, G., Sahoo, B.K.: Effect of III-V nitrides on performance of graphene based SPR biosensor for detection of hemoglobin in human blood sample: a comparative analysis. Curr. Appl. Phys. **16**, 1607–1613 (2016). https://doi.org/10.1016/j.cap.2016.09.006
Moon, B.J., Jang, D., Yi, Y., Lee, H., Kim, S.J., Oh, Y., Lee, S.H., Park, M., Lee, S., Bae, S.: Multi-functional nitrogen self-doped graphene quantum dots for boosting the photovoltaic performance of BHJ solar cells. Nano Energy **34**, 36–46 (2017)
Mostufa, S., Paul, A.K., Chakrabarti, K.: Detection of hemoglobin in blood and urine glucose level samples using a graphene-coated SPR based biosensor. OSA Contin. **4**, 2164 (2021). https://doi.org/10.1364/osac.433633

Mudgal, N., Saharia, A., Choure, K.K., Agarwal, A., Singh, G.: Sensitivity enhancement with anti-reflection coating of silicon nitride (Si_3N_4) layer in silver-based Surface Plasmon Resonance (SPR) sensor for sensing of DNA hybridization. Appl. Phys. A Mater. Sci. Process. **126**, 1–8 (2020). https://doi.org/10.1007/s00339-020-04126-9

Mukhtar, W.M., Murat, N.F., Samsuri, N.D., Dasuki, K.A.: Maximizing the response of SPR signal: a vital role of light excitation wavelength. AIP Conf. Proc. **2018**, 020104 (2016). https://doi.org/10.1063/1.5055506

Nisha, A., Maheswari, P., Anbarasan, P.M., Rajesh, K.B., Jaroszewicz, Z.: Sensitivity enhancement of surface plasmon resonance sensor with 2D material covered noble and magnetic material (Ni). Opt. Quantum Electron. **51**, 1–12 (2019). https://doi.org/10.1007/s11082-018-1726-3

Noda, Y., Hayakawa, T.: Systematic control of edge length, tip sharpness, thickness, and localized surface plasmon resonance of triangular Au nanoprisms. J. Nanopart. Res. **18**, 1–12 (2016). https://doi.org/10.1007/s11051-016-3581-0

Nur, J.N., Hasib, M.H.H., Asrafy, F., Shushama, K.N., Inum, R., Rana, M.M.: Improvement of the performance parameters of the surface plasmon resonance biosensor using Al_2O_3 and WS_2. Opt. Quantum Electron. **51**, 1–11 (2019). https://doi.org/10.1007/s11082-019-1886-9

Nuryadi, R., Mayasari, R.D.: ZnO/Au-based surface plasmon resonance for CO_2 gas sensing application. Appl. Phys. A Mater. Sci. Process. **122**, 1–6 (2016). https://doi.org/10.1007/s00339-015-9536-y

Omar, N.A.S., Fen, Y.W.: Recent development of SPR spectroscopy as potential method for diagnosis of dengue virus E-protein. Sens. Rev. (2017). https://doi.org/10.1108/SR-07-2017-0130

Omar, N.A.S., Fen, Y.W., Abdullah, J., Zaid, M.H.M., Daniyal, W.M.E.M.M., Mahdi, M.A.: Sensitive surface plasmon resonance performance of cadmium sulfidequantum dots-amine functionalized graphene oxide based thin film towards dengue virus E-protein. Opt. Laser Technol. **114**, 204–208 (2019). https://doi.org/10.1016/j.optlastec.2019.01.038

Omar, N.A.S., Fen, Y.W., Abdullah, J., Mustapha Kamil, Y., Daniyal, W.M.E.M.M., Sadrolhosseini, A.R., Mahdi, M.A.: Sensitive detection of dengue virus type 2 E-proteins signals using self-assembled monolayers/reduced graphene oxide-PAMAM dendrimer thin film-SPR optical sensor. Sci. Rep. **10**, 1–15 (2020). https://doi.org/10.1038/s41598-020-59388-3

Omar, N.A.S., Irmawati, R., Fen, Y.W., Noryana Muhamad, E., Kamal Eddin, F.B., Anas, N.A.A., Ramdzan, N.S.M., Fauzi, N.I.M., Adzir Mahdi, M.: Surface refractive index sensor based on titanium dioxide composite thin film for detection of cadmium ions. Meas. J. Int. Meas. Confed. **187**, 110287 (2022). https://doi.org/10.1016/j.measurement.2021.110287

Omidniaee, A., Karimi, S., Farmani, A.: Surface plasmon resonance-based SiO_2 Kretschmann configuration biosensor for the detection of blood glucose. SILICON **14**, 3081–3090 (2022). https://doi.org/10.1007/s12633-021-01081-9

Pal, S., Verma, A., Raikwar, S., Prajapati, Y.K., Saini, J.P.: Detection of DNA hybridization using graphene-coated black phosphorus surface plasmon resonance sensor. Appl. Phys. A Mater. Sci. Process. **124**, 1–11 (2018). https://doi.org/10.1007/s00339-018-1804-1

Pan, D., Zhang, J., Li, Z., Wu, M.: Hydrothermal route for cutting graphenesheets into blue-Luminescent graphene quantum dots. Adv. Mater. **6**, 734–738 (2010)

Panda, A., Pukhrambam, P.D., Keiser, G.: Performance analysis of graphene-based surface plasmon resonance biosensor for blood glucose and gas detection. Appl. Phys. A Mater. Sci. Process. **126**, 1–12 (2020). https://doi.org/10.1007/s00339-020-3328-8

Pandey, A.K.: Graphene–$Ti_3C_2T_x$ MXene hybrid nanostructure: a promising material for sensitivity enhancement in plasmonic sensor. Appl. Phys. A Mater. Sci. Process. **127**, 1–6 (2021). https://doi.org/10.1007/s00339-020-04235-5

Pang, P., Yan, F., Li, H., Li, H., Zhang, Y., Wang, H., Wu, Z., Yang, W.: Graphene quantum dots and Nafion composite as an ultrasensitive electrochemical sensor for the detection of dopamine. Anal. Methods **8**, 4912–4918 (2016). https://doi.org/10.1039/c6ay01254j

Pristinski, D., Kozlovskaya, V., Sukhishvili, S.A.: Determination of film thickness and refractive index in one measurement of phase-modulated ellipsometry. J. Opt. Soc. Am. A **23**, 2639 (2006). https://doi.org/10.1364/josaa.23.002639

Protich, Z., Wong, P., Santhanam, K.S.V.: Composite of zinc Using graphene quantum dot bath: a prospective material for energy storage. ACS Sustain. Chem. Eng. **4**, 6177–6185 (2016)

Qian, Z.S., Shan, X.Y., Chai, L.J., Chen, J.R., Feng, H.: Dual-colored graphene quantum dots-labeled nanoprobes/graphene oxide: Functional carbon materials for respective and simultaneous detection of DNA and thrombin. Nanotechnology **25**, 415501 (2014)

Ramdzan, N.S.M., Fen, Y.W., Anas, N.A.A., Omar, N.A.S., Saleviter, S.: Development of biopolymer and conducting polymer-based optical sensors for heavy metalion detection. Molecules **25**, 26 (2020)

Rosddi, N.N.M., Fen, Y.W., Omar, N.A.S., Anas, N.A.A., Hashim, H.S., Ramdzan, N.S.M., Fauzi, N.I.M., Anuar, M.F., Daniyal, W.M.E.M.M.: Glucose detection by gold modified carboxyl-functionalized graphene quantum dots-based surface plasmon resonance. Optik **239**, 166779 (2021). https://doi.org/10.1016/j.ijleo.2021.166779

Sadrolhosseini, A.R., Krishnan, G., Safie, S., Beygisangchin, M., Rashid, S.A., Harun, S.W.: Enhancement of the fluorescence property of carbon quantum dots based on laser ablated gold nanoparticles to evaluate pyrene. Opt. Mater. Express **10**, 2705 (2020). https://doi.org/10.1364/ome.411019

Salvi, J., Barchiesi, D.: Measurement of thicknesses and optical properties of thin films from surface plasmon resonance (SPR). Appl. Phys. A Mater. Sci. Process. **115**, 245–255 (2014). https://doi.org/10.1007/s00339-013-8038-z

Sandu, T.: Shape effects on localized surface plasmon resonances in metallic nanoparticles. J. Nanopart. Res. **14**, 1–10 (2012). https://doi.org/10.1007/s11051-012-0905-6

Schneider, T., Jahr, N., Jatschka, J., Csaki, A., Stranik, O., Fritzsche, W.: Localized surface plasmon resonance (LSPR) study of DNA hybridization at single nanoparticle transducers. J. Nanopart. Res. **15**, 1–10 (2013). https://doi.org/10.1007/s11051-013-1531-7

Shushama, K.N., Rana, M.M., Inum, R., Hossain, M.B.: Graphene coated fiber optic surface plasmon resonance biosensor for the DNA hybridization detection: simulation analysis. Opt. Commun. **383**, 186–190 (2017). https://doi.org/10.1016/j.optcom.2016.09.015

Singh, S., Prajapati, Y.K.: Highly sensitive refractive index sensor based on D-shaped PCF with gold-graphene layers on the polished surface. Appl. Phys. A Mater. Sci. Process. **125**, 1–7 (2019). https://doi.org/10.1007/s00339-019-2731-5

Singh, M.K., Pal, S., Verma, A., Das, R., Prajapati, Y.K.: A nanolayered structure for sensitive detection of hemoglobin concentration using surface plasmon resonance. Appl. Phys. A Mater. Sci. Process. **127**, 1–10 (2021). https://doi.org/10.1007/s00339-021-04985-w

Srivastava, T., Purkayastha, A., Jha, R.: Graphene based surface plasmon resonance gas sensor for terahertz. Opt. Quantum Electron. **48**, 1–11 (2016). https://doi.org/10.1007/s11082-016-0462-9

Sudhagar, P., Herraiz-Cardona, I., Park, H., Song, T., Noh, S.H., Gimenez, S., Sero, I.M., Fabregat-Santiago, F., Bisquert, J., Terashima, C., Paik, U., Kang, Y.S., Fujishima, A., Han, T.H.: Exploring graphene quantum dots/TiO_2 interface in photoelectrochemical reactions: solar to fuel conversion. Electrochim. Acta **187**, 249–255 (2016)

Sumantri, R., Hasanah, L., Arifin, M., Tayubi, Y.R., Wulandari, C., Rusdiana, D., Julian, C., Pawinanto, R.E., Susthita Menon, P., Sahari, S.K., Mulyanti, B.: Simulation of hemoglobin detection using surface plasmon resonance based on kretschmann configuration. J. Eng. Sci. Technol. **15**, 2239–2247 (2020)

Tan, F., Cong, L., Li, X., Zhao, Q., Zhao, H., Quan, X., Chen, J.: An electrochemical sensor based on molecularly imprinted polypyrrole/graphene quantum dots composite for detection of bisphenol A in water samples. Sensors Actuators, B Chem. **233**, 599–606 (2016). https://doi.org/10.1016/j.snb.2016.04.146

Tang, L., Ji, R., Li, X., Teng, K.S., Lau, S.P.: Size-dependent structural and optical characteristics of glucose-derived graphene quantum dots. Part. Part. Syst. Char. **6**, 523–531 (2013)

Tashkhourian, J., Dehbozorgi, A.: Determination of dopamine in the presence of ascorbic and uric acids by fluorometric method using graphene quantum dots. Spectrosc. Lett. **49**, 319–325 (2016). https://doi.org/10.1080/00387010.2016.1144074

Teymourinia, H., Salavati-Niasari, M., Amiri, O., Safardoust-Hojaghan, H.: Synthesis of graphene quantum dots from corn powder and their application in reduce charge recombination and increase free charge carriers. J. Mol. Liq. **242**, 447–455 (2017). https://doi.org/10.1016/j.molliq.2017.07.052

Tian, P., Tang, L., Teng, K.S., Lau, S.P.: Graphene quantum dots from chemistry to applications. Mater. Today Chem. **10**, 221–258 (2018). https://doi.org/10.1016/j.mtchem.2018.09.007

Tiwari, K., Sharma, S.C., Hozhabri, N.: High performance surface plasmon sensors: simulations and measurements. J. Appl. Phys. (2015). https://doi.org/10.1063/1.4929643

Verma, A., Prakash, A., Tripathi, R.: Performance analysis of graphene based surface plasmon resonance biosensors for detection of pseudomonas-like bacteria. Opt. Quantum Electron. **47**, 1197–1205 (2015). https://doi.org/10.1007/s11082-014-9976-1

Vijayaraghavan, K., Padmesh, T.V.N., Palanivelu, K., Velan, M.: Biosorption of nickel(II) ions ontoa Sargassum wightii: application of two-parameter and three-parameter isotherm models. J. Hazard. Mater. **133**, 304–308 (2006). https://doi.org/10.1016/j.jhazmat.2005.10.016

Wang, L., Tricard, S., Yue, P., Zhao, J., Fang, J., Shen, W.: Polypyrrole and graphene quantum dots@Prussian Blue hybrid film on graphite felt electrodes: application for amperometric determination of l-cysteine. Biosens. Bioelectron. **77**, 1112–1118 (2016). https://doi.org/10.1016/j.bios.2015.10.088

Wei, W., Nong, J., Zhang, G., Tang, L., Jiang, X., Chen, N., Luo, S., Lan, G., Zhu, Y.: Graphene-based long-period fiber grating surface plasmon resonance sensor for high-sensitivity gas sensing. Sensors. **17**, 2 (2016). https://doi.org/10.3390/s17010002

Xia, G., Zhou, C., Jin, S., Huang, C., Xing, J., Liu, Z.: Sensitivity enhancement of two-dimensional materials based on genetic optimization in surface Plasmon resonance. Sensors **19**, 1198 (2019). https://doi.org/10.3390/s19051198

Xiao, S., Zhou, D., Luan, P., Gu, B., Feng, L., Fan, S., Liao, W., Fang, W., Yang, L., Tao, E., Guo, R., Liu, J.: Graphene quantum dots conjugated neuroprotectivepeptide improve learning and memory capability. Biomaterials **106**, 98–110 (2016)

Xu, L., Zhang, S., Tan, Y., Sun, L.: Simultaneous measurement of refractive-index and thickness for optical materials by laser feedback interferometry. Rev. Sci. Instrum. **85**, 083111 (2014). https://doi.org/10.1063/1.4892465

Xu, L., Tan, Y.D., Zhang, S.L., Sun, L.Q.: Measurement of refractive index ranging from 1.42847 to 2.48272 at 1064 nm using a quasi-common-path laser feedback system. Chin. Phys. Lett. **32**, 090701 (2015). https://doi.org/10.1088/0256-307X/32/9/090701

Yan, X., Cui, X., Li, B., Li, L.-S.: Large, Solution-processable graphene quantum dots as light absorbers for photovoltaics. Nano Lett. **10**, 1869–1873 (2010a)

Yan, X., Cui, X., Li, L.-S.: Synthesis of large, stable colloidal graphene quantumdots with tunable size. J. Am. Chem. Soc. **17**, 5944–5945 (2010b)

Yan, Y., Liu, Q., Du, X., Qian, J., Mao, H., Wang, K.: Visible light photoelectrochemical sensor for ultrasensitive determination of dopamine based on synergistic effect of graphene quantum dots and TiO_2 nanoparticles. Anal. Chim. Acta **853**, 258–264 (2015). https://doi.org/10.1016/j.aca.2014.10.021

Yang, H., Wang, G., Lu, Y., Yao, J.: Highly sensitive refractive index sensor based on SPR with silver and titanium dioxide coating. Opt. Quantum Electron. **53**, 1–13 (2021). https://doi.org/10.1007/s11082-021-02981-1

Yuan, X., Liu, Z., Guo, Z., Ji, Y., Jin, M., Wang, X.: Cellular distribution and cytotoxicity of graphene quantum dots with different functional groups. Nanoscale Res. Lett. **9**, 1–9 (2014). https://doi.org/10.1186/1556-276X-9-108

Yuan, H., Ji, W., Chu, S., Qian, S., Wang, F., Masson, J.F., Han, X., Peng, W.: Fiber-optic surface plasmon resonance glucose sensor enhanced with phenylboronic acid modified Au nanoparticles. Biosens. Bioelectron. **117**, 637–643 (2018). https://doi.org/10.1016/j.bios.2018.06.042

Yuan, Y.J., Xu, Z., Chen, Y.: Investigation of dopamine immobilized on gold bysurface plasmon resonance. AIP Adv. **9**(3), 035028 (2019). https://doi.org/10.1063/1.5081869

Zhang, W., Zhang, X., Dong, X., Ma, H., Wang, G.: Synthesis of N-doped graphene oxide quantum dots with the internal P-N heterojunction and its photocatalytic performance under visible light illumination. J. Adv. Oxid. Technol. **21**, 201700331 (2018)

Zhao, J., Zhao, L., Lan, C., Zhao, S.: Graphene quantum dots as effective probes for label-free fluorescence detection of dopamine. Sensors Actuators, B Chem. **223**, 246–251 (2016). https://doi.org/10.1016/j.snb.2015.09.105

Zhou, X., Liu, K.Y., Zhang, N., Kim, D.H., Tan, C.: Nanosphere dispersion on a large glass substrate by low dose ion implantation for localized surface plasmon resonance. J. Nanopart. Res. **13**, 2919–2927 (2011). https://doi.org/10.1007/s11051-010-0182-1

Zhou, X., Ma, P., Wang, A., Yu, C., Qian, T., Wu, S., Shen, J.: Dopamine fluorescent sensors based on polypyrrole/graphene quantum dots core/shell hybrids. Biosens. Bioelectron. **64**, 404–410 (2015). https://doi.org/10.1016/j.bios.2014.09.038

Zhu, S., Zhang, J., Tang, S., Qiao, C., Wang, L., Wang, H., Liu, X., Li, B., Li, Y., Yu, W., Wang, X., Sun, H., Yang, B.: Surface chemistry routes to modulate the photoluminescence of graphene quantum dots: from fluorescence mechanism to up-conversion bioimaging applications. Adv. Funct. Mater. **22**, 4732–4740 (2012a)

Zhu, S., Zhang, J., Liu, X., Li, B., Wang, X., Tang, S., Meng, Q., Li, Y., Shi, C., Hu, R., Yang, B.: Graphene quantum dots with controllable surface oxidation, tunable fluorescence and up-conversion emission. RSC Adv. **2**, 2717–2720 (2012b)

Zhu, Z., Ma, J., Wang, Z., Mu, C., Fan, Z., Du, L., Bai, Y., Fan, L., Yan, H., Phillips, D.L., Yang, S.: Efficiency enhancement of perovskite solar cells through fast electron extraction: the role of graphene quantum dots. J. Am. Chem. Soc. **136**, 3760–3763 (2014)

Zubair, M., Mustafa, M., Ali, A., Doh, Y.H., Choi, K.H.: Improvement of solution based conjugate polymer organic light emitting diode by ZnO-graphene quantum dots. J. Mater. Sci. Mater. Electron. **26**, 3344–3351 (2015)